

# Unfurlable Offset Antenna Design for L- and C-Band Application

W. Schäfer\* and H. Herbig†

*Messerschmitt-Bölkow-Blohm GmbH, Ottobrunn, FRG*

A. Roederer‡

*European Space Research and Technology Centre, Noordwijk, The Netherlands*

and

K. Pontoppidan§

*TICRA, Copenhagen, Denmark*

Offset antennas with aperture diameters up to 12 m and a medium surface accuracy, will be required for some future European communication satellites. A special offset reflector design with deployable ribs running radially outwards from the apex and covered by a mesh will be suitable for such applications. This paper presents a parametric investigation of the rf characteristics of such an unfurlable antenna concept with single mesh as described above. For a 4.5-m-diam reflector (4/6 GHz application) a lightweight mechanical design has been elaborated based on the design principle already shown. Main features of this reflector and the deployment principle are given.

## Introduction

**I**N a recent survey of mission opportunities and technology requirements<sup>1</sup> performed at the European Space Agency, deployable satellite antennas have been identified as a critical technology item for several European space applications in the next two decades.

Multibeam, low side lobe, low cross-polarization applications require offset-fed reflectors with root mean square (rms) surface tolerances of the order of a hundredth of a wavelength for diameters of 10-200 wavelengths pointed with accuracies of up to a few hundredths of a degree.

For frequencies above 6 GHz, requiring very tight reflector surface tolerances, several designs, at various stages of development, are available or being studied mainly in the United States, but also in Europe. Most of them, however, have been specified for symmetrical center-fed configurations and only a few of the available concepts can readily be modified for nonsymmetrical offset-fed configurations.<sup>2,3</sup> For frequencies below 6 GHz, absolute surface tolerance requirements are less stringent and can, in many cases, be met by a single-mesh unfurlable design.

The range of the reflector diameter considered extends from 4 to about 12 m, the lower limit results from the available stowage diameter of ARIANE IV and Space Shuttle (antennas with smaller diameters do not need an unfurlable reflector), the upper limit from the expected achievable beam pointing accuracies (a few hundredths of a degree).

Offset-fed configurations are required for most multibeam applications. Designs capable of meeting the above low-frequency and offset requirements are not available in Europe, and have not been, to the authors' knowledge, described in open literature.

Furthermore, the impact of surface deviations and of the choice of mesh configuration on side lobe and cross-

polarization performance must be studied to assess the limitations of single-mesh offset reflector antennas.

For this reason, a study was initiated to define and evaluate one (or more) suitable design(s) compatible with the ARIANE IV launcher and with the European L-SAT type platform.<sup>4</sup> The objective of this paper is to present the results of this preliminary study, in particular, the case of an offset 4.5-m, 4-GHz antenna.

## Main Requirements and Interfaces for a Model Antenna

For the study presented, some antenna specifications have been assumed, the most important of which are as follows:

Launcher: ARIANE IV (3.65 m dynamic envelope diameter).

Platform: L-SAT.

Reflector configuration: deployable (unfurlable) offset reflector mounted on the east side of the platform; circular projected aperture; clearance ( $D/3$ ) between focal axis and reflector edge to allow for feed or subreflector mounted on tower;  $F/D$  in the range 0.8-1.2 to allow for reasonable off-axis beam performance.

Type of design: unfurlable mesh reflecting surface; single offset for smaller diameters; dual offset for larger diameters; compatible with fine pointing mechanism.

Most critical environmental specifications: stiffness and eigenfrequency requirements, respectively, compatible with L-SAT (see Table 1).

The model antenna investigated had an aperture diameter of 4.5 m, but the design concept selected had to be extendable up to about 12 m diameter.

## Analysis of Different Possible Reflector Design Concepts

### Reflector Design Principles under Investigation

Two quite different reflector design principles have been compared with regard to the special antenna requirements. They are: 1) rib concepts with reflective mesh, especially radial rib approach (concept with deployable or extendable mast) and fan rib concept (concept by which ribs are running outward from the vertex); and 2) spatial framework design with adjustable reflective mesh, especially the parabolic erectable truss antenna (PETA) concept from General Dynamics.

Presented as Paper 82-0443 at the AIAA 9th Communication Satellite Systems Conference, San Diego, Calif., March 7-11, 1982; submitted April 1, 1982; revision received May 6, 1983. Copyright © American Institute of Aeronautics and Astronautics, Inc., 1982. All rights reserved.

\*Senior Engineer, Antenna Structures, Space Division.

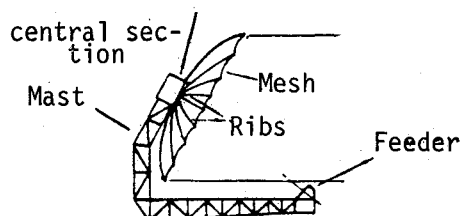
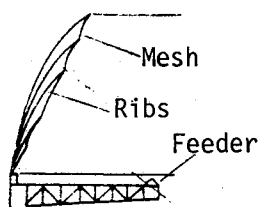
†Design Engineer, Spacecraft Structures, Space Division.

‡Senior Research Engineer, Spacecraft Antennas.

§Senior Research Engineer, Antennas.

**Table 1 Most critical mechanical environmental specifications (stiffness and eigenfrequency, respectively)**

Requirement	Specified value	
Sinusoidal vibration	Frequency, Hz	Acceleration, g
Longitudinal axis	17-60	13
Lateral axis	18-45	15
Stiffness	Resonance frequency, Hz	
Longitudinal axis	>60	
Lateral axis	>45	

**Fig. 1 Offset reflector radial rib concept (principle).****Fig. 2 Offset reflector fan rib concept (principle).****Short Description of the Rib Concepts****Radial Rib Approach (Fig. 1)**

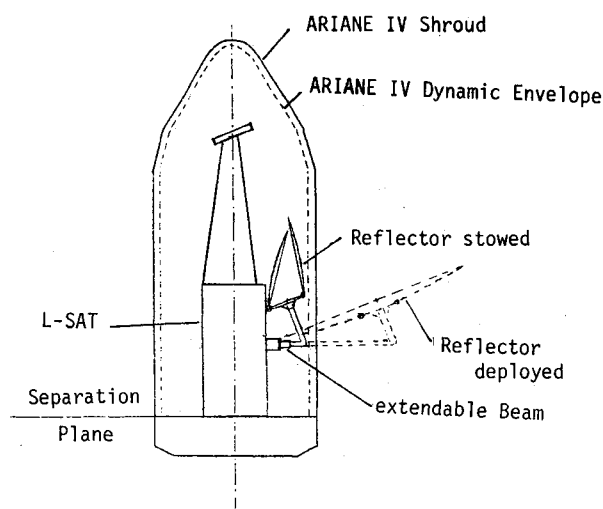
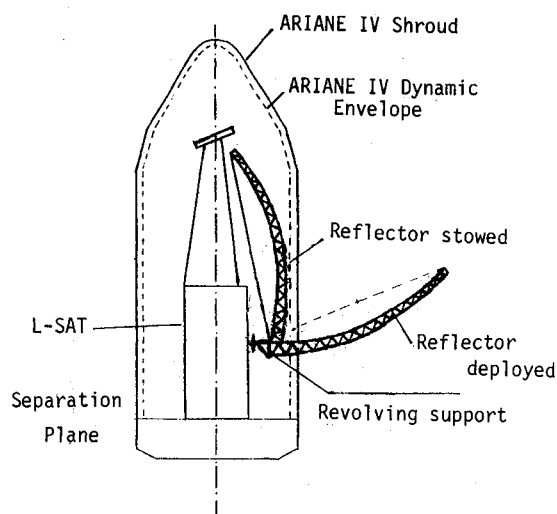
The basic structure of the reflector includes the ribs, the rigid central section, deployment mechanism, and an extendable beam; while the rf reflective surface is formed by a metallic tricot mesh. The offset radial rib concept uses the radial rib system attached to a central section, as in the well-known axisymmetric design concepts, except that the central section is not located in the symmetry center. The carbon fiber reinforced plastics (CFRP) ribs support and help shape the mesh; because of the asymmetry each rib has a different shape. The mechanical deployment system provides a controlled deployment from the stowed to the fully deployed position. In order to be compatible with the geometrical interfaces an extendable beam also will be required.

**Fan Rib Concept (Fig. 2)**

The basic structure of the reflector includes the ribs, the revolving support, and the deployment mechanism; the rf reflective surface is formed by a metallic tricot mesh. The CFRP ribs are protruding from the vertex of the paraboloid and they are folded like a fan. They support and help shape the reflective mesh, the two most outward ribs on both sides are joined together rigidly in order to get a stiff element for the reflector rim. A motor-driven deployment system first deploys the fan by means of the revolving support and then provides a controlled deployment of the ribs up to the final position.

**Short Description of the PETA Concept (see Ref. 2)**

The reflector support structure consists of a number of basic structural elements used in numerous combinations to achieve the desired shape and size of the antenna. The basic element is a deployable tetrahedron truss that is hinged by spider links at each corner. Each tetrahedron forms one truss bay, which can vary in number across the major diameter of

**Fig. 3 Deployable offset radial rib reflector in ARIANE IV-shroud (L-SAT interface).****Fig. 4 Deployable offset fan rib reflector in ARIANE IV-shroud (L-SAT interface).**

the reflector structure. This configuration is the basis of the support structure for the rf reflective mesh. Deployment of the basic tetrahedron is made possible by hinging the struts at their centers with carpenter tape. This type of hinge provides for zero slope, while maintaining sufficient strain energy to accomplish deployment and an excellent mechanical lockup in the deployed configuration.

**Selection of Most Suitable Reflector Design Concept**

Assuming a reflector mounting on the east panel of the satellite, the reflector framework concept cannot be mounted on L-SAT, because a very large stowage diameter of the cylindrical stowage volume (about 1 m) is required. Therefore only rib concepts have been considered further.

Figures 3 and 4 show the geometrical constraints for the radial rib reflector principle and fan rib concept, respectively. The radial rib concept needs an extendable, thermally stable beam while the fan rib concept only needs a revolving support. This revolving support can be used also for fine pointing of the reflector. An advantage of the radial rib concept is better adaptation of the mesh surface approximation to the illumination function of the surface. Both rib concepts can be stowed under the shroud on the satellite's east panel. Primarily because of the additional expandable beam required, the fan rib concept has been selected.

### Electrical Performance of Fan Rib Offset Reflector Concept

The reflector surface may be constructed as single or dual mesh. In the single-mesh design the mesh is attached only to the ribs, while the surface between the ribs is part of a parabolic cylinder. In the dual-mesh design the reflecting front mesh is connected to a drawing mesh on the rear side by means of a large number of adjustable ties. In this way a good approximation to the perfect paraboloidal shape may be obtained. This solution clearly has a large impact on complexity and manufacturing costs. The single-mesh concept will give rise to a degradation of the main beam gain and to increased side lobes. In many practical cases, however, these effects are small. An investigation of the rf characteristics of a single-mesh offset fan rib antenna is presented as follows. The aim will be to classify the unfurlable antennas into two groups: one in which the single-mesh construction is sufficient, and another in which the dual-mesh solution is mandatory.

#### Circular Symmetric Configuration

The symmetrical equivalent to the offset fan rib design is the so-called umbrella reflector. The main-beam performance for this antenna has been investigated theoretically by Ingerson and Wong<sup>5</sup> and experimentally by Imbriale et al.<sup>6</sup> More recently the side lobes have been investigated by Rusch and Wanselow.<sup>7</sup>

Figure 5 shows a comparison of the radiation pattern of a  $100\lambda$  paraboloid with that of the equivalent umbrella reflector with 20 gores.<sup>7</sup> The  $f/D$  of the paraboloid of the umbrella is 0.4. The pattern plane is the symmetry plane of a gore. The feed is excited in circular polarization and the amplitude pattern is  $\cos\theta$ . For the smooth paraboloid the feed is located at the focal point, and for the umbrella antenna the feed is located at the focal point for the best fit paraboloid. From Fig. 5 the following three effects of the gores can be seen: 1) the peak gain is reduced, 2) the first side lobes are reduced, and 3) high side lobes are introduced from about  $\theta = 3.5$  deg.

The analysis of Rusch and Wanselow involves only one gore (due to the quasirotational symmetry) and the patterns are expressed in terms of Bessel functions. From these expressions one can derive that the high-gore side lobe will start at any angle  $\theta_g$  given approximately by

$$\pi(D/\lambda)\sin\theta_g = N_g \quad (1)$$

where  $N_g$  is the number of gores (or ribs). For  $N_g = 20$  this gives  $\theta_g = 3.65$  deg. It is assumed that the surface within each gore is a parabolic cylinder whose focal length is

$$f_g = f \cos^2(\pi/N_g) \quad (2)$$

and the focal length for the best fit paraboloid is<sup>6</sup>:

$$f_{bfp} = f[1 - (2\pi^2/3N_g^2)] \quad (3)$$

In order to understand the phenomena for the offset radial rib antenna, it is desirable to have a simpler interpretation of the results in Fig. 5. This can be obtained by a geometrical theory of diffraction (GTD) consideration by means of Fig. 6. For the paraboloidal reflector the side lobes are created by interference between the diffracted rays from points  $P_1$  and  $P_2$ , assuming that the pattern plane is the  $XZ$  plane and no other diffraction points are present. Also, for the umbrella antenna,  $P_1$  and  $P_2$  will be diffraction points, but the diffractions will be smaller because the umbrella antenna has no axial caustic. This is the reason for the lower near inside lobes previously mentioned in point 2. However, for the umbrella antenna also, points  $Q_1$  and  $Q_2$  on two neighboring gore segments will be possible diffraction points. The distance between  $Q_1$  and  $Q_2$  is  $D\sin(\pi/N_g)$ . For increasing  $\theta$ , the angle from boresight, the diffractions from  $Q_1$  and  $Q_2$  will add in

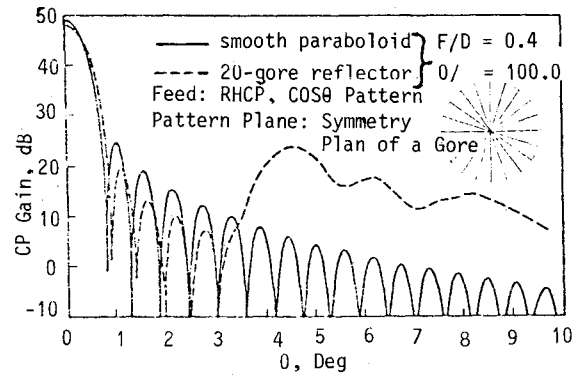


Fig. 5 Comparison of radiation pattern for paraboloid and umbrella reflector with 20 gores.

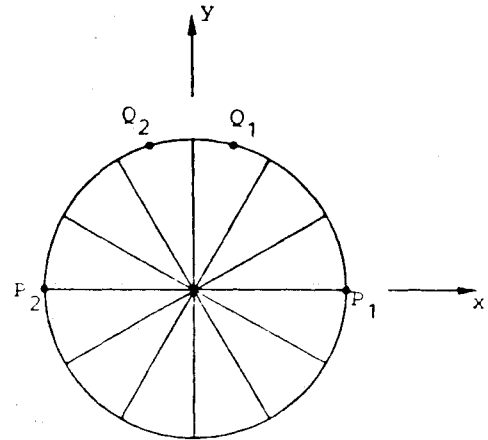


Fig. 6 Diffraction points for an umbrella antenna.

phase for the first time when the distance to the far field differs by one wavelength. This happens when  $D\sin(\pi/N_g)\sin\theta = \lambda$ , which is practically identical to Eq. (1).

The preceding simple and approximate analysis shows why the gore-related side lobes do not interfere with the first side lobes of the antenna pattern. Equation (1) also shows that if the number of gores is increased the gore-related side lobes will begin at a higher value of  $\theta$ , whereas the radiation pattern in the central section remains almost the same as that of the perfect paraboloid.

#### Offset Fan Rib Configuration

The offset fan rib antenna is shown in Fig. 7. The focal length of the parent paraboloid is  $f$  and the diameter of the antenna aperture is  $D$ . The clearance between the lower edge of the reflector and the axis is  $d_c$ . The ribs are separated by the angle  $\alpha$ . For the calculations to be presented subsequently, an  $f/D$  ratio of unity has been selected. An indication of the effect of other values of  $f/D$  will be given. The clearance is  $d_c = D/3$ , which allows the reflector dish to be mounted on the side of a spacecraft whereas the feed is located on the top platform. The reflector surface is exactly the same as for the rotational symmetric case but it is only an offset part of the surface which is used. The feed is excited in the circular polarization and tilted upwards toward the reflector. The radiation pattern of the feed is rotationally symmetric and the amplitude pattern is given by

$$10^{-A/20}(\theta/\theta_0)^2 \quad (4)$$

where  $A$  is the feed taper in decibels at the angle  $\theta_0$ .

The radiation characteristics of the fan rib antenna will be investigated for the feed at focus as well as for the feed displaced from the focus.

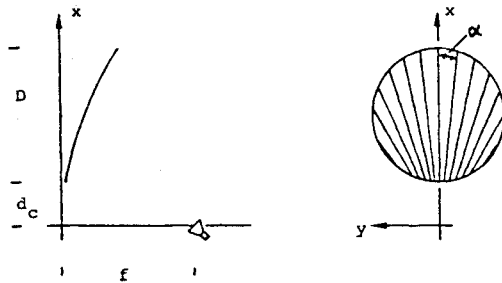


Fig. 7 Offset fan rib antenna.

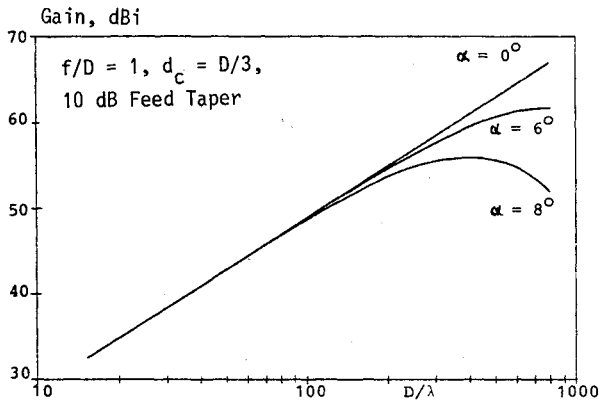


Fig. 8 Peak gain for offset fan rib antenna.

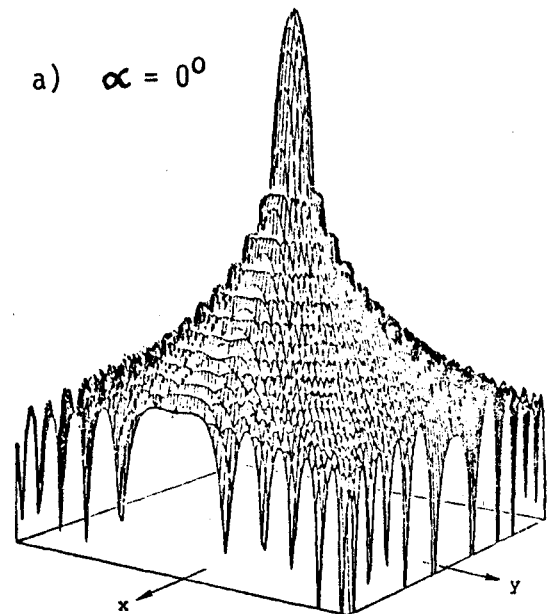
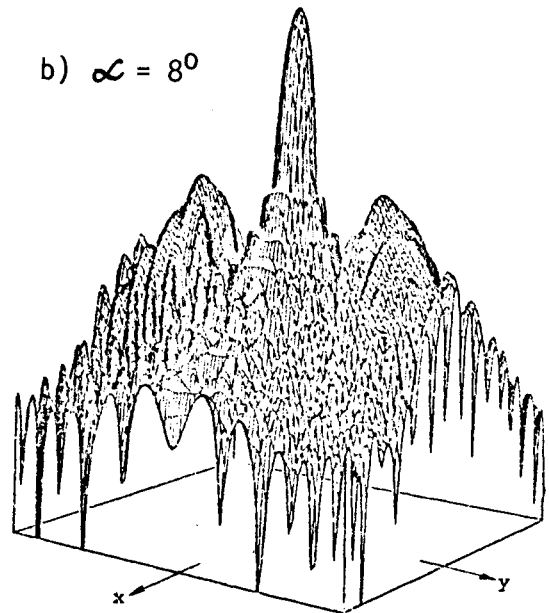
#### Feed at Focus

The feed is located at the focal point for the best fit paraboloid as given by Eq. (3) where  $N_g$  is related to the angle  $\alpha$  between the ribs by  $N_g = 2\pi/\alpha$ .

The deviations from a paraboloidal surface give rise to a degradation of the peak gain. This is illustrated in Fig. 8 where the peak gain is plotted for the smooth paraboloid,  $\alpha = 0$  deg, as well as for  $\alpha = 6$  and  $8$  deg. This result shows that for  $D/\lambda \leq 100$  the gain loss due to the ribs is negligible. For  $D/\lambda > 100$ , Fig. 8 can be used for a tradeoff between different mechanical configurations. If, for example, a peak gain of 55 dB is desired this can be obtained with a smooth paraboloid (using a dual-mesh configuration) and  $D = 200\lambda$ . However, the same peak gain is obtained with a single mesh with  $\alpha = 6$  deg and  $D = 215\lambda$  or with  $\alpha = 8$  deg and  $D = 250\lambda$ . It is seen that the gain loss decreases rapidly when the angular distance between the ribs is reduced. Fan rib designs for  $\alpha > 8$  deg are probably not feasible for mechanical reasons.

For many applications the side lobe structure is of special importance. For the rotationally symmetric antenna it was shown that the ribs rise to side lobes for  $\theta > \theta_g$ , where  $\theta_g$  is given by Eq. (1). The first gore-related side lobes will, for the offset antenna in Fig. 7, be due to diffraction points on neighboring gores on the top edge and this means that they will appear primarily in the plane of asymmetry,  $\phi = 90$  deg. This is verified in Fig. 9 which shows a three-dimensional plot of the complete radiation pattern in the region near the main beam. For comparison the pattern for a smooth paraboloidal reflector is also shown. Figure 10 shows the pattern cuts corresponding to Fig. 9 for the plane of symmetry,  $\phi = 0$  deg, and the plane of asymmetry,  $\phi = 90$  deg.

Equation (1) can still be used to predict the position at which the gore side lobes start to dominate but in the offset case the value of  $D$  should be replaced by twice the distance from the top edge to the axis. For the case in Fig. 10,  $\theta_g = 3.1$  deg is in good agreement with the calculated pattern. The results clearly show that the rib structure does not perturb the side lobes of the smooth reflector in the plane of symmetry and the same is true for the plane of asymmetry for  $\theta < \theta_g$ .

b)  $\alpha = 8^\circ$ Fig. 9 Radiation diagram for smooth reflector.  $D/\lambda = 100$ ,  $f/D = 1$ ;  $d_c = D/3$ , 10 dB feed taper.

During the design phase it may be necessary to select  $\alpha$  such that  $\theta_g$  is sufficiently large. Applying Eq. (1) for the offset configurations gives

$$\alpha = \frac{1}{(D + d_c/\lambda) \sin \theta_g} \quad (5)$$

If, for example, the gore-related side lobes in Fig. 10b should be pushed from 3.9 to 6.2 deg the value of  $\alpha$  should be reduced from 8 to 4 deg. This shows that the side-lobe specification can have a great impact on the mechanical structure.

During the preceding analysis the  $f/D$  ratio was unity. If  $f/D$  is decreased the deviations of the rib surface from the smooth paraboloid will be larger. This means that the peak gain loss and the amplitude of the gore-related side lobes will increase. The position of the side lobes, however, will remain unchanged.

It has also been assumed that the surface within each gore is a parabolic cylinder. However, a mesh attached to curved ribs

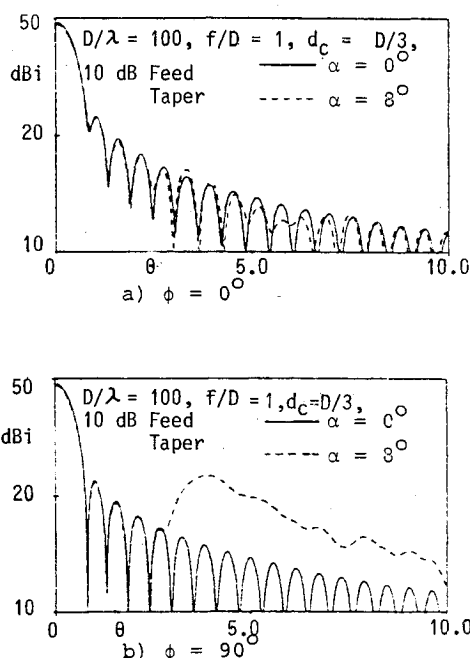


Fig. 10 Principal plane radiation patterns for smooth reflector.

will produce an out-of-plane motion commonly referred to as "pillow." The effect of pillow is very similar to a reduction of the  $f/D$  ratio, but a preliminary analysis has indicated that the influence for realistic configurations is quite small.

#### Scanning Performance

When the feed is offset from the focal point the radiation pattern will suffer from a reduction in gain and increased side lobes. The aim of the following will be to demonstrate, by example, that the scanning performance of the fan rib antenna is not inferior to that of a smooth paraboloidal reflector surface. The example in question is:  $D=100\lambda$ ,  $f/D=1$ ,  $d_c=D/3$ ,  $\alpha=8$  deg. The patterns for the focus-fed configuration are shown in Fig. 10.

Figure 11 shows the pattern in the plane of asymmetry when the beam has been tilted about 4.7 beamwidths in the same plane. Again it is seen that within the region of the gore-related side lobes the pattern for the fan rib design is identical to that of the smooth paraboloid. In other words, the rib structure does not deteriorate the scanning performance.

### Detailed Design of a 4.5 m Unfurlable Offset Reflector (Fan Rib Concept)

#### Overall Design

The fan rib concept selected and analyzed concerning rf properties has been designed in more detail. The principle of the design and its deployment sequence can be taken from Fig. 12. Figures 13-15 show some details of the launch and orbit configuration (the numbers are in millimeters). The main features of the design are:

Geometrically nearly identical ribs (except the reinforced central rib), different only in length, made in CFRP.

Reflective mesh connected to the ribs with standoffs on the ribs which are adjustable (exact parabolic shape along the ribs only).

Connection between satellite sidewall and the reflector itself by means of a revolving reflector support, made from a tubular CFRP framework.

Controlled deployment with cables, connected to the articulated levers and driven by motor.

The calculated eigenfrequency of the fan rib reflector in the stowed position is slightly above 50 Hz. The reflector supporting structure consists of ribs. The main middle rib is

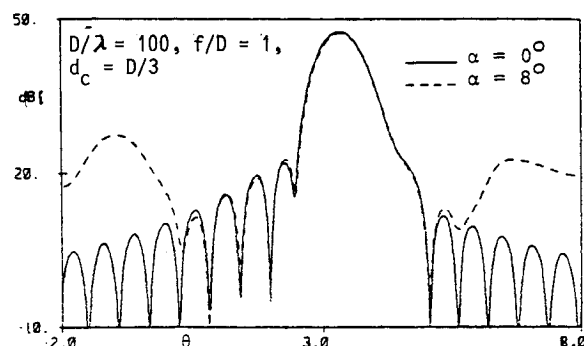


Fig. 11 Radiation pattern in plane of asymmetry with beam tilted 4.7 beamwidths.

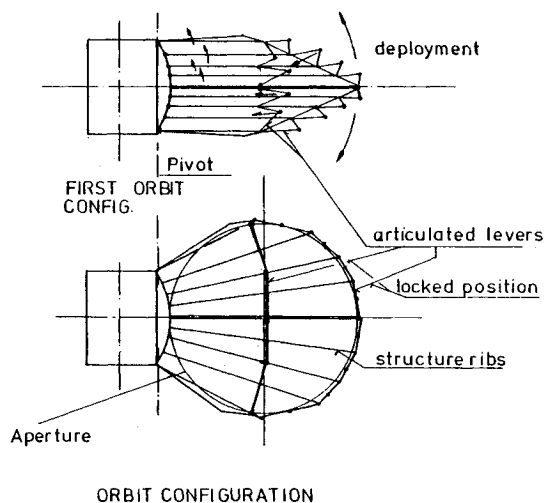
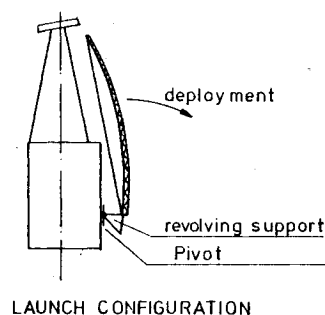


Fig. 12 Design principle and deployment sequence of the offset fan rib reflector concept.

stiffly connected to the revolving support. This rib has been designed very stiff in view of a relatively high eigenfrequency requirement. Lowering the eigenfrequency requirement allows a simpler main rib design (all ribs except the outer-ribs plane). The other ribs are connected rotating with the revolving support, such that folding of the reflector is possible.

The ribs do not have an exactly parabolic shape, such that the exactly parabolic shape of the reflective mesh surface along the rib has to be adjusted with standoffs connected to the ribs. The mesh is connected to the standoffs. Attached to the ribs are the hinges for articulated levers. These levers are connected with the deployment mechanism. Between the ribs and attached to the ribs are box-shaped elements for a stiff connection of the ribs in the stowed position.

#### Reflector Components

##### Revolving Support

The reflector support is designed as a revolving support.

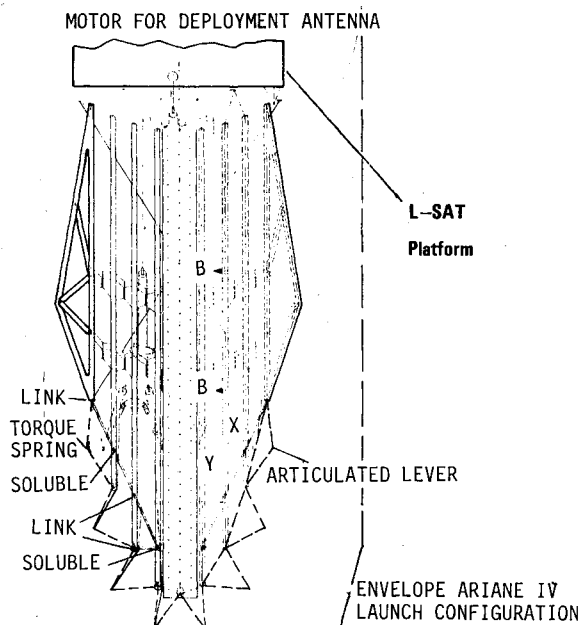


Fig. 13 Fan rib reflector concept (first orbit position).

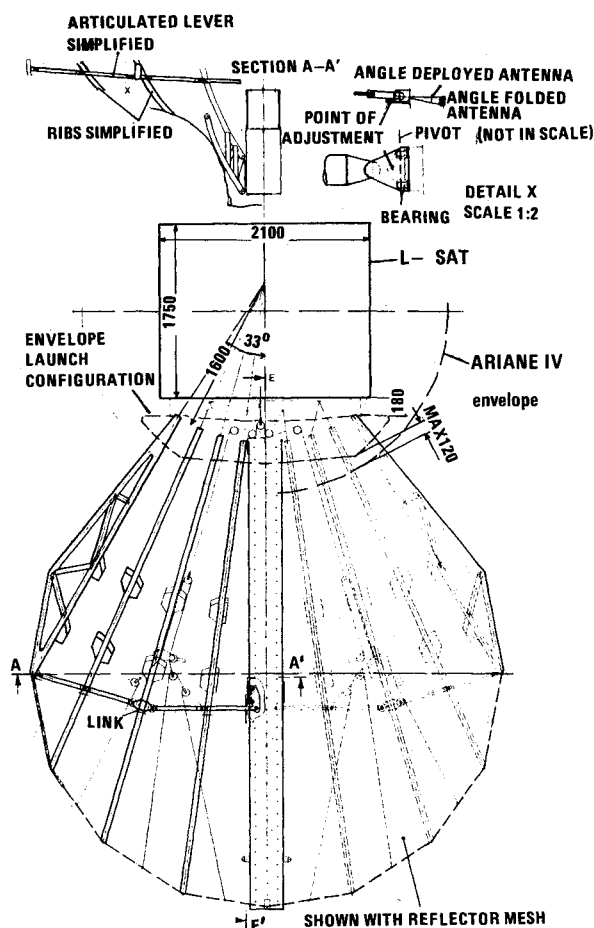


Fig. 14 Fan rib reflector concept (final orbit position = deployed position).

The support consists of a CFRP tube framework. The connection of the middle rib with the support frame can be seen in Fig. 16.

The support is rotary supported in the pivot hinges which are connected to the satellite's surface. The support can be turned around the pivot from launch to orbit position (Fig. 17).

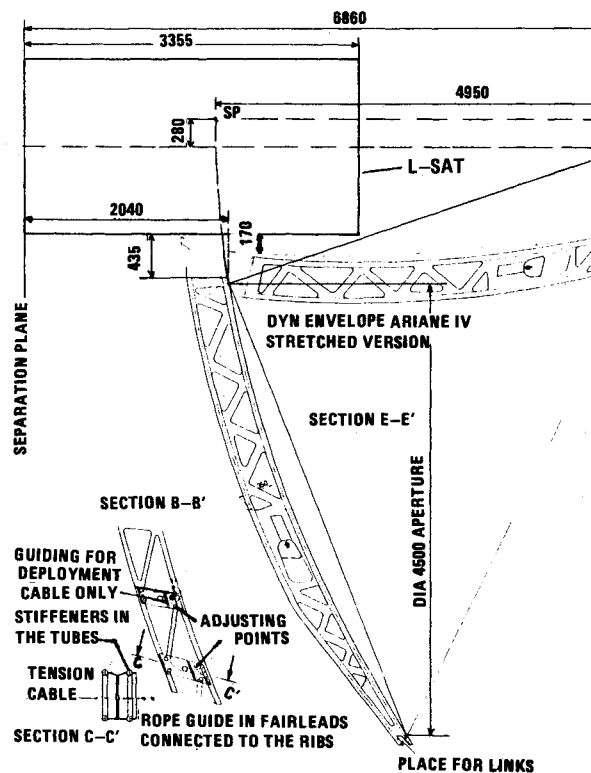


Fig. 15 Fan rib reflector concept (main middle rib).

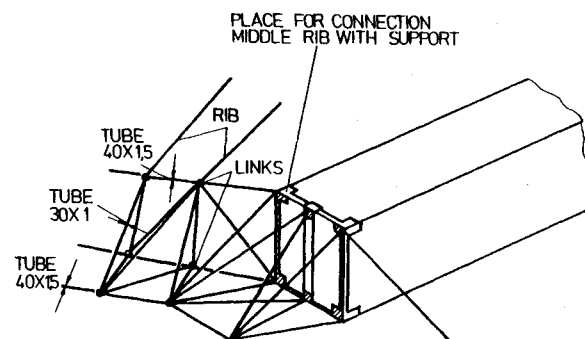


Fig. 16 Middle rib connection with support, e.g., screws, bolts.

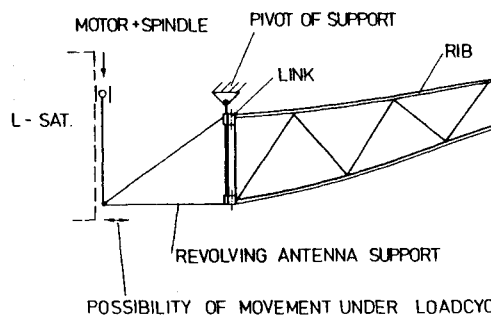


Fig. 17 Functional principle of the revolving support providing for antenna pointing.

A motor with, for example, harmonic drive gear or a stepper motor drives a spindle. A nut is mounted at this spindle which is connected to the revolving support tubes with hinges. By means of this mechanism the support can be turned from launch to orbit position. In orbit position the support may be locked by the motor. Motors and cable rolls of the deployment mechanism are mounted to the revolving support.

### Structure of Ribs

The reflector structure consists of three different types of ribs:

1) The middle rib. This rib has to stiffen the whole reflector structure in launch configuration. Furthermore, it has to transmit the forces of the articulated levers during the deployment phase. The rib structure consists of a box-shaped CFRP sandwich construction. The connection links for the articulated levers are made of titanium. They are connected to the ribs. The middle rib is connected to the support by means of inserts (Fig. 16).

2) Revolving ribs (inner ribs). These ribs consist of a plane CFRP-tube framework. They are designed for low weight at high stiffness. The connection points of the articulated levers have to be stiffened and the hinges of these levers have to be fastened with titanium inserts.

3) Outside ribs. These two ribs are built of a triangular CFRP framework. The design was selected in order to get high stiffness in all directions during launch and in orbit. The inner part of these ribs will be made in the same manner as the revolving ribs. The ribs are completed with additional tubes and stiffeners to the final triangular configuration.

### Deployment, Release, and Hold-down Mechanisms

**Deployment Mechanism.** The deployment mechanism consists of articulated levers made of CFRP driven by a motor. They are arranged close to the middle section of the reflector and at the tips of the ribs (see Figs. 13 and 14). The levers in the middle section have a locking device to ensure that the reflector diameter will not change in orbit.

The tension cables work, in principle, like a winding tackle to open the reflector fan. They are rolled up by means of a motor which is designed such that after antenna deployment the cables roll out for several millimeters (no tension forces by the cables under critical thermal conditions).

**Hold-down Mechanism.** The hold-down mechanism consists of three parts. These are:

1) The two rows of chainings (see section B-B' and C-C' in Fig. 15). Function: In the launch configuration the reflector ribs with the chaining plates are pressed together by means of a tensioned cable (cable 1). The plates are centered with a cone (section C-C') and the two rows are connected with a cable.

2) The triangular chaining with soluble links from the top of the reflector to the tip of the triangular ribs. Function (see Fig. 14, detail X): In the launch configuration, a bolt, held down and fixed by cable 2, connects the tubes of the chaining in the soluble links. If cable 2 has been cut, the bolt is pressed out of the connection of the tubes by spring force and the chaining will open.

3) A tension cable (cable 3) to give higher stiffness to the reflector fan. It is situated between the triangular ribs and the revolving support. This chaining also shall limit the high accelerations at the tips of the ribs (about 120 g).

**Cable Cutting.** One end of the cables is connected to the middle rib, the other end to the cable cutter. The cables are guided in rope guidings, the diameter of the stainless steel cable is 1 mm. After cutting, the cables remain in the rope guidings during the deployment of the reflector. Each cable has a knot or a pressed ball at the open side of the cutter.

### Mesh System

The knitted reflector mesh is made of 50- $\mu$ -thick gold-plated molybdenum wire. It is connected to the ribs with adjustable stand-offs. At the reflector rim the mesh requires stiffeners to avoid the pillow effect. In addition, stiffeners will be required for a well-defined reflector mesh folding.

### Reflector Thermal Control

In order to minimize thermal distortion of the ribs they are covered with thermal blankets. The thickness of the thermal

**Table 2** Mass budget for the unfurlable offset reflector (fan rib concept)

Reflector ribs (without middle rib), articulated levers, chainings	32.0 kg
Reflector revolving support	7.0 kg
Standoffs, hinges, axis, middle rib	5.2 kg
Reflector mesh	1.2 kg
Motor + spindle	1.0 kg
Cables from stainless steel	6.3 kg
Cables from Kevlar	(1.2 kg)
Total reflector mass (including revolving support)	
Stainless steel cables	52.7 kg
Kevlar cables	47.6 kg

blanket applied depends upon the thermal requirements, 5-10 mm thickness is a reasonable range resulting in a very good thermal insulation of the ribs. The revolving support will be covered by a thermal blanket also.

### Mass Budget

The mass budget for the deployable offset reflector with 4.5 m aperture diam and a minimum eigenfrequency > 50 Hz is shown in Table 2.

### Conclusions

The gores of the offset fan rib antenna give rise to side lobes which do not disturb the radiation near the main beam. The position of the gore-related side lobes moves away from the main beam as the angular spacing between the ribs is decreased. It is concluded that as long as the side lobe specifications refer only to the pattern up to a certain region from boresight, the angular spacing between the ribs can be adjusted so that the gore-related side lobes fall outside this region. The gore effect reduces the peak gain, but this effect is small and can be compensated by a slight increase in the reflector diameter. The fan rib design does not deteriorate the scanning performance as compared to a smooth reflector. A relatively simple mechanical design of the fan rib concept has been elaborated which fulfills the requirements of minimum thermal distortion (orbit position), as well as a minimum first eigenfrequency of 50 Hz (stowed position) for the reflector at a relatively low overall mass (47.6 kg for the 4.5 m reflector). This could be achieved only by extensive use of CFRP for the rib support structure and by using a tricot mesh made of gold-plated molybdenum wires for the reflective surface. The antenna does not need any deployable mast, the reflector is deployed by means of a motor-driven controlled deployment mechanism. The overall reflector mass may be reduced considerably if eigenfrequency requirements are reduced.

### References

- <sup>1</sup>Stoewer, H., Capart, J.J., Mica, G., and Whitcomb, G., "The New Approach to the Definition of the ESA Technological Research Programme," *ESA Bulletin*, No. 24, Nov. 1980, pp. 63-67.
- <sup>2</sup>Freeland, R.E., "Industry Capability for Large Space Antenna Structures," Jet Propulsion Laboratory, Rept. 710-12, May 25, 1978.
- <sup>3</sup>Schäfer, W., "Stand der Technik auf dem Gebiet grösserer entfaltbarer Parabolantennen-Strukturen für Raumfluggeräte," *Zeitschrift Flugwiss. Weltraumforschung*, Vol. 4, Sept./Oct. 1980, pp. 255-267.
- <sup>4</sup>Roederer, A. and Festa, A., "Study of Offset Unfurlable Antennas," Technical Specifications and Statement of Work, ESA AO/1-1264/80/NL/MS, July 1980.
- <sup>5</sup>Ingerson, P.G. and Wong, W.C., "The Analysis of Deployable Umbrella Parabolic Reflectors," *IEEE Transactions on Antennas and Propagation*, Vol. AP-20, 1972, pp. 409-414.
- <sup>6</sup>Imbriale, W.A., Ingerson, P.G., and Wong, W.C., "Experimental Verification of the Analysis of Umbrella Parabolic Reflectors," *IEEE Transactions on Antennas and Propagation*, Vol. AP-21, 1973, pp. 705-708.
- <sup>7</sup>Rusch, W.V.T. and Wanselow, R.D., "Gore-related Sidelobes of an Umbrella Reflector," *IEEE International Symposium*, Quebec, 1980, AP-S, Vol. II, pp. 481-484.